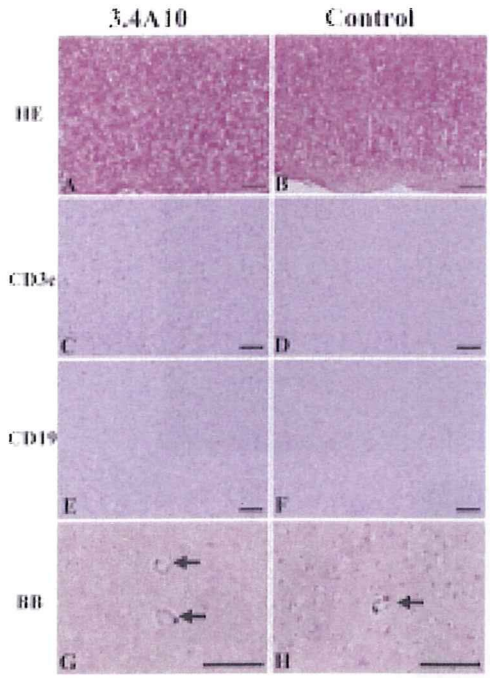

Fig. 5. No lymphocytic infiltration and slight but not significant increase of microhemorrhage in the brain sections. Staining with HE (A, B), Berlin blue (G, F) and antibodies against CD3e (C, D) and CD19 (E, F) in the sagittal brain sections of the Tg2576 mice. The arrows in G and F show the Berlin blue positive vessels. Left panel, 3.4A10 therapeutic group; right panel, control group. Scale bar = 100 μm. HE, hematoxylin and eosin stain; BB, Berlin blue stain.

one branch of immunotherapy, unlike active immunization, the passive immunization would not elicit undesired cellular responses, and more importantly, it allows us to monitor the antibody titer to modify the dosage and frequency of antibody infusion in order to avoid any adverse effects that might follow the passive administration of antibody without consideration whether the vaccine could arouse the immune response or not individually. Previous studies showed that anti-Aβ antibodies that effectively reduced amyloid burden had the following features: 1) ability to stain senile plaques rather than bind soluble Aβ; and 2) epitope location within N-terminus of Aβ [1,2,18]. Moreover, the TAPIR antibody was related to the slower decline of cognitive functions in AD patients who received active immunization [10].

The obtained anti-human Aβ mouse monoclonal antibody, 3.4A10, was selected by ELISA, but further immunohistochemical staining showed its ability to recognize senile plaques. The results of detection of Aβ fragments by 3.4A10 with dot blot and western blot simulated the patterns of anti-Aβ_{1-42} C-terminal specific antibodies, however, the competitive Biacore analysis showed that 3.4A10 only blocked the binding of 6E10, an anti-Aβ N-terminal antibody, to the sensor chip without inhibiting the binding of other two antibodies that recognize the middle portion and C-terminal portion of Aβ. We concluded that epitope of 3.4A10 is located in the N-terminal portion of Aβ. And the ability of 3.4A10 to inhibit Aβ_{1-42} aggregation on the ThT spectrophotometry assay further confirmed this conclusion as previously reported that N-terminal 3–6 amino acid residues EFRH of Aβ were presented as the epitope of its anti-aggregating antibodies [6]. More interestingly, 3.4A10 had higher affinity to Aβ_{1-42} than to Aβ_{1-40}, and this was consistent with the dot blot and western blot results that 3.4A10 detected Aβ_{1-42} better than Aβ_{1-40}, as well as the immunohistochemical staining results that 3.4A10 recognized less plaque cores which contained mainly Aβ_{1-40} [17]. Similarly, we also found that 3.4A10 immunoreactivities were rarely co-localized with von Willebrand factor-positive blood vessels in AD brain samples (data not shown). We termed 3.4A10 as a TAPIR-like antibody due to above mentioned characteristics in addition to the fact that it did not recognize native or denatured AβPPs.

We also evaluated the therapeutic effects of 3.4A10 in a small number of 18 months old Tg2576. As expected, 3.4A10 significantly decreased the amyloid burden in brain after 8 weeks treatment by a quantitative image analysis. We also measured the Aβ_{40} and Aβ_{42} contents in the brain lysates by a sensitive sandwich ELISA assay. As 3.4A10 had more affinity to Aβ_{42} than to Aβ_{40}, 3.4A10 significantly reduced the Aβ_{42} levels compared to the control group, while less interfered with Aβ_{40} levels. It was suggested that the extracellular soluble Aβ*56 (12mer), a 56-kD Aβ assembly impaired memory independently of plaques or neuron loss [16]. 3.4A10 therapy diminished the Aβ*56 levels in the soluble fraction of brain lysates by a western blot analysis.

The major adverse effect of passive anti-Aβ antibody therapy in the mouse model of AD is the increased incidence of microhemorrhage due to the age-related cerebral amyloid angiopathy (CAA) [25,26]. Tg2576 mouse model of AD carries Swedish mutation of AβPP under control of hamster prion protein promoter, and was found that Aβ_{1-40} is the predominant amyloid deposit component [12]. The selective increase of Aβ_{1-40} results in development of high levels of CAA and related cerebral microhemorrhage [25]. We investigated the microhemorrhage in the 3.4A10-treated mice and control mice, and found that there was slight but not significant increase in microhemorrhage.

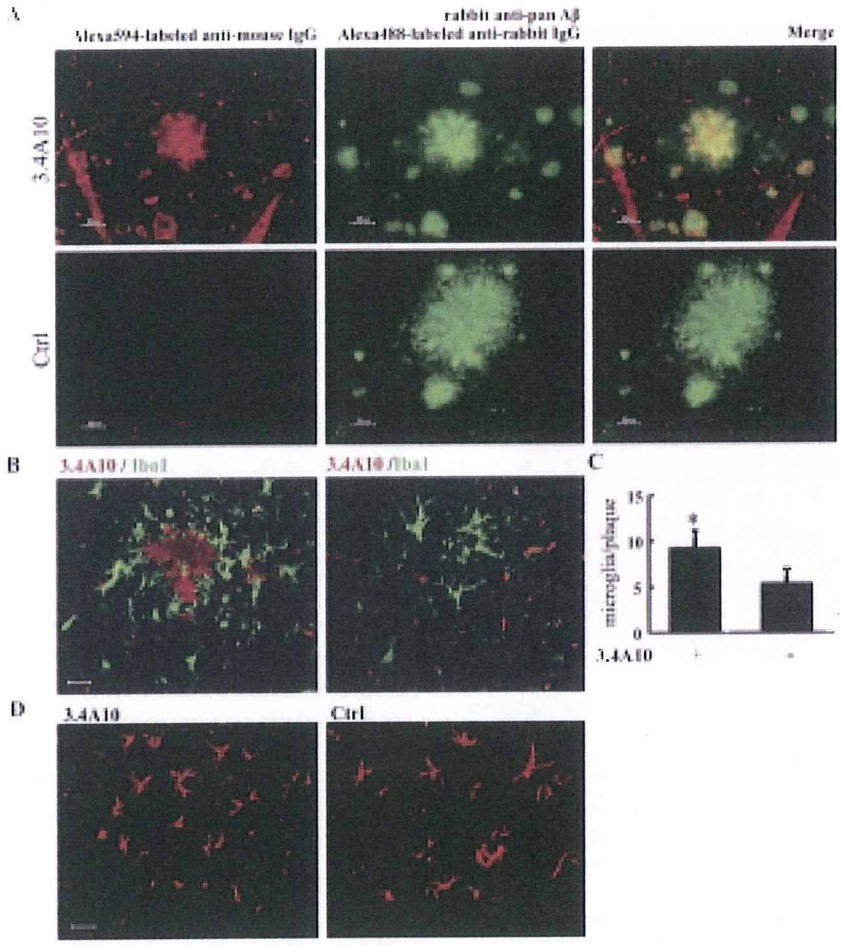

Fig. 6. 3.4A10 entered the brain and decorated some plaques which were surrounded with more Iba1-positive microglia. A) That 3.4A10 entered the brain was elucidated by direct staining of the sections with Alexa 594-labeled donkey anti-mouse IgG antibody. The 3.4A10 decorated plaques (red) were colocalized with rabbit anti-pan Aβ antibody stained ones (green) as shown in the upper panel of A. Alexa 594-labeled donkey anti-mouse IgG antibody did not stain any plaque in the brain sections of the control group as shown in lower panel of A. Bar = 25 μm. B) 3.4A10 decorated plaques (red) were surrounded more Iba1-positive microglia (green) than 3.4A10 negative plaques in the 3.4A10 therapeutic group, bar = 20 μm. C) The numbers of microglia per plaque were compared between 3.4A10 positive and negative plaques in the 3.4A10 therapeutic group. $^*p < 0.001$. D) There was no difference in GFAP-positive astrocytes between the two groups, bar = 20 μm.

This negative result may be due to the lower affinity of 3.4A10 to $A\beta_{1-40}$ and should be interpreted prudently. Meningoencephalitis was also reported to associate with passive immunization [15], but we did not see any inflammatory changes by HE staining and immunohistochemical staining for T and B lymphocytes.

There have been three hypotheses used to explain how antibodies reduced Aβ deposition [31]. One is that the direct effect of antibody on Aβ, leading to dissolution of amyloid fibrils [6,14,30]. The second hypothesis is that anti-Aβ antibody induces Fc receptor (FcR)-mediated phagocytosis of Aβ by microglia [1, 27]. The third one is termed as peripheral sink hypothesis, postulates that anti-Aβ antibody in the circulation leads to a net efflux of Aβ from brain to plasma [5]. Our results suggested that all of these three possible mechanisms might contribute to the decreased amyloid burden by 3.4A10 therapy. 3.4A10 degraded the $A\beta_{1-42}$ fibrils *in vitro*; 3.4A10 entered the brain and decorated some senile plaques which were surrounded by more Iba1-positive microglia; 3.4A10 therapy increased the serum $A\beta_{42}$ levels by a quantitative ELISA assay (data not shown).

Although the clinical trial was halted, Aβ immunotherapy would still be a potential therapeutic or preventive approach for AD. 3.4A10, the antibody we developed in this study, recognizes N-terminal portion of Aβ with a different affinity to Aβ species ($A\beta_{1-42}$ >

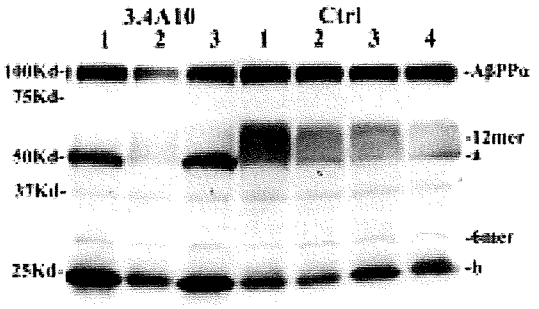

Fig. 7. Western blot results of Aβ oligomers in TBS fraction of the brain lysates. Compared to the control, the 3.4A10 reduced the 12mer Aβ oligomer without obvious effects on other Aβ oligomer. The sAβPP and amyloid oligomers were detected by 6E10 and HRP conjugated goat anti-mouse IgG second antibody. a, immunoglobulin heavy chain; b, immunoglobulin light chain.

$A\beta_{1-40}$), and more importantly it recognizes the senile plaques without binding the native or denatured form of AβPPs. The animal experiment showed its ability to decrease brain amyloid burden in a relatively short period (8 weeks) without any obvious side effects related to immunotherapy as previous reported. Further intensive study should be performed in order to provide some insights for selecting anti-Aβ antibodies for AD treatment.

ACKNOWLEDGMENTS

This work was supported in part by grand in aid for Scientific Research on Priority Area (17025056) from the Ministry of Education, Culture, Science and Technology. We Thank Dr. K. Takahashi, H. Wakida, A. Watanaba, A. Sekiyama, K. Takeda, K. Yoshizaki, K. Adachi and H.Y. Liu for their kind help and discussion in this work.

References

[1] F. Bard, C. Cannon, R. Barbour, R.L. Burke, D. Games, H. Grajeda, T. Guido, K. Hu, J. Huang, K. Johnson-Wood, K. Khan, D. Kholodenko, M. Lee, I. Lieberburg, R. Motter, M. Nguyen, F. Soriano, N. Vasquez, K. Weiss, B. Welch, P. Seubert, D. Schenk and T. Yednock, Peripherally administered antibodies against amyloid β-peptide enter the central nervous system and reduce pathology in mouse model of Alzheimer's disease, *Nat Med* **6** (2000), 916–919.

[2] F. Bard, R. Barbour, C. Cannon, R. Carretto, M. Fox, D. Games, T. Guido, K. Hoenow, K. Hu, K. Johnson-Wood, K. Khan, D. Kholodenko, C. Lee, M. Lee, R. Motter, M. Nguyen, A. Reed, D. Schenk, P. Tang, N. Vasquez, P. Seubert and T. Yednock, Epitope and isotype specificities of antibodies to beta-amyloid peptide for protection against Alzheimer's disease-like neuropathology, *Proc Natl Acad Sci USA* **100** (2003), 2023–2028.

[3] R. Bullock, Future directions in the treatment of Alzheimer's disease, *Expert Opin Investig Drugs* **13** (2004), 303–314.

[4] J.L. Cummings, Alzheimer's disease, *N Engl J Med* **351** (2004), 56–67.

[5] R.B. DeMattos, K.R. Bales, D.J. Cummins, J.C. Dodart, S.M. Paul and D.M. Holtzman, Peripheral anti-Aβ antibody alters CNS and plasma Aβ clearance and decreases brain Aβ burden in a mouse model of Alzheimer's disease, *Proc Natl Acad Sci USA* **98** (2001), 8850–8855.

[6] D. Frenkel, M. Balass and B. Solomon, N-terminal EFRH sequence of Alzheimer's β-amyloid pepetide represents the epitope of its anti-aggregating antibodies, *J Neuroimmunol* **88** (1998), 85–90.

[7] S. Gilman, M. Koller, R.S. Black, L. Jenkins, S.G. Griffith, N.C. Fox, L. Eisner, L. Kirby, M.B. Rovira, F. Forette and J.M. Orgogozo, AN1792(QS-21)-201 Study Team, Clinical effects of Abeta immunization (AN1792) in patients with AD in an interrupted trial, *Neurology* **64** (2005), 1553–1562.

[8] H. Hara, A. Monsonego, K. Yuasa, K. Adachi, X. Xiao, S. Takeda, K. Takahashi, H.L. Weiner and T. Tabira, Development of a safe oral Abeta vaccine using recombinant adeno-associated virusvector for Alzheimer's disease, *J Alzheimers Dis* **6** (2004), 483–488.

[9] C. Hock, U. Konietzko, A. Papassotiropoulos, A. Wollmer, J. Streffer, R.C. Von Rotz, G. Davey, E. Moritz and R.M. Nitsch, Generation of antibodies specific for β-amyloid by vaccination of patients with Alzheimer disease, *Nat Med* **8** (2002), 1270–1275.

[10] C. Hock, U. Konietzko, J.R. Streffer, J. Tracy, A. Signorell, B. Muller-Tillmanns, U. Lemke, K. Henke, E. Moritz, E. Garcia, M.A. Wollmer, D. Umbricht, D.J. de Quervain, M. Hofmann, A. Maddalena, A. Papassotiropoulos and R.M. Nitsch, Antibodies against beta-amyloid slow cognitive decline in Alzhiemer's disease, *Neuron* **38** (2003), 547–554.

[11] C. Janus, J. Pearson, J. McLaurin, P.M. Mathews, Y. Jiang, S.D. Schmidt, M.A. Chishti, P. Home, D. Heslin, J. French, H.T. Mount, R.A. Nixon, M. Mercken, C. Bergeron, P.E. Fraser, P. St George-Hyslop and D. Westaway, A beta peptide immunization reduces behavioural impairment and plaques in a model of Alzheimer's disease, *Nature* **408** (2000), 979–982.

[12] T. Kawarabayashi, L.H. Younkin, T.C. Saido, M. Shoji, K.H. Ashe and S.G. Younkin, Age-dependent changes in brain, CSF, and plasma amyloid β protein in the Tg2576 transgenic mouse model of Alzheimer's disease, *J Neurosci* **21** (2001), 372–381.

[13] H.W. Klafki, M. Staufenbiel, J. Kornhuber and J. Wiltfang, Therapeutic approaches to Alzheimer's disease, *Brain* **129** (2006), 2840–2855.

[14] I. Klyubin, D.M. Walsh, C.A. Lemere, W.K. Cullen, G.M. Shankar, V. Betts, E.T. Spooner, L. Jiang, R. Anwyl, D.J. Selkoe and M.J. Rowan, Amyloid β protein immunotherapy neutralizes Aβ oligomers that disrupt synaptic plasticity *in vivo*, *Nat Med* **11** (2005), 556–561.

[15] E.B. Lee, L.Z. Leng, V.M. Lee and J.Q. Trojanowski, Meningoencephalitis associated with passive immunization of a transgenic murine model of Alzheimer's amyloidosis, *FEBS Lett* **579** (2005), 2564–2568.

[16] S. Lesne, M.T. Koh, L. Kotilinek, R. Kayed, C.G. Glabe, A. Yang, M. Gallagher and K.H. Ashe, A specific amyloid-β protein assembly in brain impairs memory, *Nature* **440** (2006), 352–357.

[17] C.L. Master, G. Simms, N.A. Weinman, G. Multhaup, B.L. McDonald and K. Beyreuther, Amyloid plaque core protein in

Alzheimer disease and Down syndrome, *Proc Natl Acad Sci USA* **82** (1985), 4245–4249.

[18] J. Mclaurin, R. Cecal, M.E. Kierstead, X. Tian, A.L. Phinney, M. Manea, J.E. French, M.H. Lambermon, A.A. Darabie, M.E. Brown, C. Janus, M.A. Chishti, P. Horne, D. Westaway, P.E. Fraser, H.T. Mount, M. Przybylski and P. St George-Hyslop, Thearpeutically effective antibodies against amyloid-beta peptide target amyloid residues 4–10 and inhibit cytotoxicity and fibrillogenesis, *Nat Med* **8** (2002), 1263–1269.

[19] D. Morgan, D.M. Diamond, P.E. Gottschall, K.E. Ugen, C. Dichey, J. Hardy, K. Duff, P. Jantzen, G. DiCarlo, D. Wilcock, K. Connor, J. Hatcher, C. Hope, M. Gordon and G.W. Arendash, A beta peptide vaccination prevents memory loss in an animal model of Alzheimer's disease, *Nature* **408** (2000), 982–985.

[20] A. Mouri, Y. Noda, H. Hara, H. Mizoguchi, T. Tabira and T. Nabeshima, Oral vaccination with a viral vector containing Abeta cDNA attenuates age-related A beta accumulation and memory deficits without causing inflammation in a mouse Alzheimer model, *FASEB J* **21** (2007), 2135–2148.

[21] J.A. Nicoll, D. Wilkinson, C. Holmes, P. Steart, H. Markham and R.O. Weller, Neuropathology of human Alzheimer disease after immunization with amyloid-beta peptide: a case report, *Nat Med* **9** (2003), 448–452.

[22] R.L. Nussbaum and C.E. Ellis, Alzheimer's disease and Parkinson's disease, *N Engl J Med* **348** (2003), 1356–1364.

[23] J.M. Orgogozo, S. Gilman, J.F. Dartigues, B. Laurent, M. Puel, L.C. Kirby, P. Jouanny, B. Dubois, L. Eisner, S. Flitman, B.F. Michel, M. Boada, A. Frank and C. Hock, Subacute meningoencephalitis in a subset of patients with AD after Aβ42 immunization, *Neurology* **61** (2003), 46–54.

[24] R.L. Patton, W.M. Kalback, C.L. Esh, T.A. Kokjohn, G.D. Van Vickle, D.C. Luehrs, Y.M. Kuo, J. Lopez, D. Brune, I. Ferrer, E. Masliah, A.J. Newel, T.G. Beach, E.M. Gastano and A.E. Roher, Amyloid-β peptide remnants in AN-1972-immunized Alzheimer's disease patients, *Am J Pathol* **169** (2006), 1048–1063.

[25] M. Pfeifer, S. Boncristiano, L. Bondolfi, A. Stalder, T. Deller, M. Staufenbiel, P.M. Mathews and M. Jucker, Cerebral hemorrhage after passive anti-Aβ immunotherapy, *Science* **298** (2002), 1379.

[26] M.M. Racke, L.I. Boone, D.L. Hepburn, M. Parsadainian, M.T. Bryan, D.K. Ness, K.S. Piroozi, W.H. Jordan, D.D. Brown, W.P. Hoffman, D.M. Holtzman, K.R. Bales, B.D. Gitter, P.C. May, S.M. Paul and R.B. DeMattos, Exacerbation of cerebral amyloid angiopathy-associated microhemorrhage in amyloid precursor protein transgenic mice by immunotherapy is dependent on antibody recognition of deposited forms of amyloid β, *J Neurosci* **25** (2005), 629–636.

[27] D. Schenk, R. Barbour, W. Dunn, G. Gordon, H. Grajeda, T. Guido, K. Hu, J. Huang, K. Johnson-Wood, K. Khan, D. Kholodenko, M. Lee, Z. Liao, I. Lieberburg, R. Motter, L. Mutter, F. Soriano, G. Shopp, N. Vasquez, C. Vandevert, S. Walker, M. Wogulis, T. Yednock, D. Games and P. Seubert, Immunization with amyloid-β attenuates Alzheimer-disease like pathology in the PDAPP mouse, *Nature* **400** (1999), 173–177.

[28] D.J. Selkoe and D. Schenk, Alzheimer's disease: Molecular understanding predicts amyloid-based therapeutics, *Annu Rev Pharmacol Toxicol* **43** (2003), 545–584.

[29] B. Solomon, R. Koppel, E. Hanan and T. Katzav, Monoclonal antibodies inhibit in vitro fibrillar aggregation of Alzheimer β-amyloid peptide, *Proc Natl Acad Sci USA* **93** (1996), 452–455.

[30] B. Solomon, R. Koppel, D. Frankel and E. Hanan-Aharon, Disaggregation of Alzheimer β-amyloid by site-directed mAb, *Proc Natl Acad Sci USA* **94** (1997), 4109–4112.

[31] H.L. Weiner and D. Frenkel, Immunology and immunotherapy of Alzheimer's disease, *Nat Rev Immunol* **6** (2006), 404–416.

Tohoku J. Exp. Med., 2008, **215**, 43-54

Juzen-taiho-to, an Herbal Medicine, Activates and Enhances Phagocytosis in Microglia/Macrophages

HUAYAN LIU,[1,2] JUN WANG,[1,2] ATSUO SEKIYAMA[1] and TAKESHI TABIRA[1]

[1]Department of Vascular Dementia Research, National Institute for Longevity Sciences, National Center for Geriatrics and Gerontology, Obu, Japan
[2]Department of Neurology, First Affiliated Hospital, China Medical University, Shenyang, P.R. China

Microglia are the main resident immunocompetent and phagocytic cells in the central nervous system (CNS). Activated microglia could play phagocytic roles as well as mediate inflammatory processes in the CNS. Involvement of activated microglia in the pathogenesis has been demonstrated in several neurological diseases including Alzheimer's disease (AD). Juzen-taiho-to (JTT), a traditional herbal medicine, has been reported to have effects on activating immune responses and phagocytosis. So far, little is known about the effects of this Kampo formulation JTT on microglia and in AD. In this report, we studied the effects of JTT on the activation and phagocytic functions of mouse microglia and bone marrow-derived macrophages (BMM). JTT could activate microglia, which was confirmed by the prominent morphological change and increased surface expression of an activation marker CD11b. In addition, JTT was revealed to induce microglial proliferation, and enhance microglial phagocytosis of, without eliciting an excessive production of nitric oxide. Furthermore, when mice were administrated with JTT in vivo, their BMM showed more effective phagocytosis of fibrillar $A\beta_{1\text{-}42}$. These findings implicate the therapeutic potential of JTT in AD and other neurological diseases accompanied by microglial activation. ——— Juzen-taiho-to (JTT); microglia/macrophages; Alzheimer's disease (AD); phagocytosis; amyloid.

Tohoku J. Exp. Med., 2008, **215** (1), 43-54.

Microglia are considered resident immune cells of myeloid origin, that take up residence in the central nervous system (CNS) during embryogenesis (Cuadros and Navascues 1998). They are regarded as CNS macrophages, and many studies gave evidence that immune reaction and inflammation related with microglia play essential roles in the pathological mechanism of some neurodegenerative diseases such as Alzheimer's disease (AD), multiple sclerosis, and so on (Rogers et al. 1988; Raine 1994). Activated microglia have been demonstrated to play the phagocytic role with extracellular β-amyloid deposits in AD (Kopec and Carroll 1998; Weldon et al. 1998). Therefore, microglia might be a therapeutic target for AD.

Juzen-taiho-to (Shi-Quan-Da-Bu-Tang in Chinese, JTT), a traditional herbal medicine, has traditionally been administered to patients with anemia, anorexia, or fatigue. From the pharmaco-

Received February 18, 2008; revision accepted for publication March 12, 2008.
Correspondence: Takeshi Tabira, National Institute for Longevity Sciences, National Center for Geriatrics and Gerontology, 36-3 Genko, Morioka, Obu 474-8511, Japan.
e-mail: tabira@nils.go.jp

logic view, JTT contains various immunomodulatory substances. For example, ginsenoside Rh1 has anti-allergic and anti-inflammatory activities (Park et al. 2004); glycyrrhizin extracted from Glycyrrhizae Radix and the extracts of Astragali Radix have anti-inflammatory activities (Shon and Nam 2003; Matsui et al. 2004); the extracts from Ginseng Radix, Cinnamomi Cortex, Glycyrrhizae Radix, Radix Paeoniae, and Astragali Radix have anti-oxidative activities (Dhuley 1999; Baltina 2003; Keum et al. 2003; Lee et al. 2003; Wang et al. 2003). Furthermore, recent studies demonstrated that ginsenosides Rg3 and Rh2 inhibited the production of nitric oxide (NO), iNOS and pro-inflammatory cytokines TNF-α, IL-1β in activated microglia (Bae et al. 2006). These results raised the possibility that the Kampo formulation JTT might have an immunomodulatory effect on microglia/macrophages, and might show its therapeutic potential in neurodegenerative diseases accompanied by microglial activation, such as AD.

In this study, we examined the effects of JTT on the activation and phagocytic functions of microglia and bone marrow-derived macrophages (BMM), as well as its effects on the production of NO in microglia.

Materials and Methods

Reagents

Synthetic human A$\beta_{1\text{-}42}$ peptide was purchased from Peptide Institute, Inc. (Osaka). Fibrillar A$\beta_{1\text{-}42}$ (fAβ_{42}) was obtained by dissolving the synthetic human peptide firstly in DMSO and then in Dulbecco's PBS (250 μM) followed by incubating at 37°C for 7 days. Lipopolysaccharide (LPS) from Escherichia coli 055: B5 was purchased from Sigma-Aldrich (St. Louis, MO, USA). Fluorescein isothiocyanate (FITC)-conjugated rat anti-mouse CD11b monoclonal antibody was purchased from BD Biosciences Pharmingen (San Jose, CA, USA). Rabbit anti-Iba1 (ionized calcium binding adaptor molecule 1) polyclonal antibody was purchased from Wako Pure Chemicals Industries, Inc. (Osaka). Mouse anti-human Aβ monoclonal antibody: 4G8 was purchased from Chemicon International, Inc. (Temecula, CA, USA). Rabbit anti-Lysosome-associated membrane protein (LAMP)-2 polyclonal antibody was purchased from Santa Cruz Biotechnology, Inc. (Santa Cruz, CA, USA). Recombinant mouse granulocyte macrophage-colony stimulating factor (GM-CSF) and recombinant mouse macrophage-colony stimulating factor (M-CSF) were from R & D Systems (Minneapolis, MN, USA).

Preparation of JTT

JTT, purchased from Tsumura and Co. (Tokyo), was composed of 10 medical plants (Table 1). JTT was prepared as follows. A mixture of Astragali Radix (3.0 g), Cinnamomi Cortex (3.0 g), Angelicae Radix (3.0 g), Paeoniae Radix (3.0 g), Cnidii Rhizoma (3.0 g), Rehmanniae Radix (3.0 g), Ginseng Radix (3.0 g), Atractylodis Lanceae Rhizoma (3.0 g), Poria (3.0 g), and Glycyrrhizae Radix (1.5 g) was added to 285 ml of water and extracted at 100°C for 1 hr. The extracted solution was filtered and spray-dried to obtain the dry extract powder (2.3 g).

Table 1. The ratio of crude drugs of Juzen-taiho-to (JTT)

Crude drugs	Ratio
Astragali Radix (*root of Astragalus membranaceus Bunge*)	3.0
Cinnamomi Cortex (*bark of Cinnamomum cassia Blume*)	3.0
Angelicae Radix (*root of Angelica acutiloba Kitagawa*)	3.0
Paeoniae Radix (*rhizome of Paeonia lactiflora Pallas*)	3.0
Cnidii Rhizoma (*rhizome of Cnidium officinale Makino*)	3.0
Rehmanniae Radix (*root of Rehmannia glutinosa Liboschitz var. purpurea Makino*)	3.0
Ginseng Radix (*root of Panax ginseng C.A. Meyer*)	3.0
Atractylodis Lanceae Rhizoma (*rhizome of Atractylodes lancea De Candolle*)	3.0
Poria (*scletrotium of Poria cocos Wolf*)	3.0
Glycyrrhizae Radix (*root of Glycyrrhiza uralensis Fischier*)	1.5

Preparation of the JTT mixture culture medium

JTT extract powder was dissolved in Dulbecco's Modified Eagle's Medium (DMEM, Sigma) by stirring at room temperature for 1 hr at a concentration of 2 mg/ml. After dissolved, it was sonicated for 30 min (Branson Sonifier 250, Danbury, CT, USA), and centrifuged at 3,000 rpm for 10 min (J6-HC Centrifuge, Beckman Coulter, Fullerton, CA, USA) to remove the insoluble materials. The supernatant was then filtered with a disposable syringe filter with a 0.22 μm PVDF membrane (Millipore, Cork, Ireland). This solution was then added with 10% fetal bovine serum (FBS, ICN Biomedicals, Aurora, OH, USA), 0.2% glucose and 5 μg/ml bovine insulin to prepare the JTT mixture culture medium.

Preparation and culture of primary microglia and Ra2 cell lines

Mouse primary microglia were isolated from primary mixed glial cell cultures obtained from newborn C57BL/6 mice by the "shaking off" method as described previously (Suzumura et al. 1987). In brief, after the meninges were carefully removed under microscope, the brains were dissociated by passing it through a 258-μm-pore nylon mesh. The cell suspension was washed twice with Hank's balanced salt solution, triturated and placed in 75-cm^2 culture flasks at a density equivalent of two brains per flask in 10 ml DMEM supplemented with 10% FBS, 0.2% glucose and 5 μg/ml bovine insulin. On the 14th day, the mixed glial cell cultures were put into Bio Shaker (TAITEC, BR-43FM, Koshigaya), and were shaken at 37°C, 150 rpm for 3 hrs. The medium was collected, centrifuged, and the harvested cells were incubated at 37°C, 5% CO_2 for 30 min. The attached cells were harvested by cell scraper. The morphological change was observed under an Olympus IX70 microscope (Olympus, Tokyo) and recorded with a Nikon digital camera DXM1200F (Nikon, Tokyo). The purity of cultured microglia was 97-100% as determined by indirect immunofluorescence staining with antibody to Iba1.

The microglial cell line Ra2 cells established from neonatal C57BL/6J (H-2^b) mice using a non-enzymatic and non-virus-transformed procedure (Sawada et al. 1998) were kindly provided by Dr. Sawada (Department of Brain Function, Research Institute of Environmental Medicine, Nagoya University, Nagoya). Ra2 cells proliferated in the same culture medium as primary microglia supplemented with 1 ng/ml GM-CSF. Before experiment, the Ra2 cells were cultured without GM-CSF for 16 hrs.

Preparation and culture of bone marrow-derived macrophages (BMM)

12-week-old female C57BL/6 wild type mice were used in this experiment. This experiment was performed under the guidelines for Animal Experiments of National Center for Geriatrics and Gerontology and approval of the institute's ethical committee for animal experiment. 8 mice were randomly divided into two groups. One group (experimental group, n = 4) was given drinking water containing 100 mg/ml of JTT. The dose was determined according to our previous study (Hara et al. unpublished). The drinking water was prepared by the similar protocol with the preparation of JTT mixture culture medium mentioned above. Since 20% of JTT was removed by the procedure of sedimentation during the preparation and each animal consumed 3 ml of the drinking water per day, the average consumption of JTT was estimated as 250 mg/day/caput. If animals spill over about 20% of drinking water, this is about 100 times higher than the dosage for human use. The other group (control group, n = 4) was given plain drinking water. After 21 days, isolation of BMM was performed by a modified method published by Takahashi and collaborators (Takahashi et al. 2007). In detail, the mice were sacrificed by decapitation and bone marrow cells were freshly flushed from the medullary cavities of the femurs and tibias with a 25 ga needle, and then filtered through a 40 μm nylon mesh. Removal of erythrocytes was performed by lysis with hypotonic solution, followed by washing twice with Dulbecco's PBS containing 2% FBS. The cells were then resuspended in DMEM containing 10% FBS and 10 ng/ml M-CSF in 75-cm^2 culture flasks. After 24 hrs, non-adherent cells were collected and re-seeded in fresh 75-cm^2 culture flasks. Medium was changed every three days, and BMM were collected for fAβ_{42}-phagocytosis assay after 12 - 13 days. The purity of BMM was more than 95% as determined by indirect immunofluorescence staining with antibody to Iba1.

Cell proliferation (WST-1) assay

Primary microglia at a density of 2 × 10^4 cells/well were plated onto a 96-well microtiter plate. Different concentrations of JTT (10, 50, 100, 200, 400 and 600 μg/ml) or LPS (0.1 μg/ml) as positive control were added to the culture medium for 48 hrs. Cell proliferation assay was determined by the PreMix WST-1 cell proliferation assay system (TaKaRa, Tokyo). This assay bases on the cleavage of tetrazolium salts which were added into the medium. These teterazolium salts are cleaved to forma-

zan dye by succinate-tetrazolium reductase, which exists in the mitochondrial respiratory chain and is active only in viable cells. At the end of the experiments, 10 μl/well PreMix WST-1 reagent was added followed by incubating at 37°C, 5% CO_2 for 4 hrs. The absorbance at the wavelength of 450 nm was measured by a microplate reader (model 550, Bio-Rad Laboratories, Hercules, CA, USA).

Flow cytometric assay

Ra2 cells were treated with different concentrations of JTT (200 and 400 μg/ml) or LPS (0.1 μg/ml) for 48 hrs. The cells were detached and single cell suspensions were made in fluorescence activated cell sorting (FACS) buffer consisting of Dulbecco's PBS containing 4% FBS and 0.1% sodium azide. The cells were then incubated with FITC-conjugated rat anti-mouse CD11b monoclonal antibody for cell surface staining at 4°C for 30 min. After washed twice with FACS buffer to remove the antibody completely, the samples were examined by FACSCalibur flow cytometer (BD, Franklin Lakes, NJ, USA) and analyzed using the Cellquest™ software (BD immunocytometry system, CA, USA).

Immunofluorescence staining for fAβ_{42}-phagocytosis assay

Both primary microglia in vitro pre-treated with different concentrations of JTT (100, 200, 400 or 600 μg/ml) for 24 hrs or pre-treated with 200 μg/ml JTT for different time periods (12, 24 or 48 hrs) and BMM from two groups which were in vivo pre-administrated with or without 100 mg/ml JTT were used for fAβ_{42}-phagocytosis assay. At the end of each treatment, the culture medium was changed and fAβ_{42} was added to a final concentration of 1 μM, followed by incubation for further 3 hrs. After fixation with 4% paraformaldehyde at 4°C for 15 min, the cells were blocked and permeabilized with PBS containing 5% normal donkey serum, 0.5% bovine serum albumin and 0.2% Triton X-100 at room temperature for 1 h. Microglia or BMM were then stained with anti-Iba1 antibody (1 : 250) or anti-LAMP-2 antibody (1:250), and fAβ_{42} was stained with 4G8 antibody (1:500) at 4°C overnight. After 3-time washes with PBS, specific binding was detected using secondary antibodies: Alexa 488-conjugated donkey anti-rabbit IgG and Alexa 594-conjugated donkey anti-mouse IgG (Molecular Probes, Eugene, OR, USA). After washing, the fluorescence was observed by an Olympus IX70 microscope equipped with appropriate filters. The fAβ_{42}-phagocytosed microglia in each group were counted in at least three randomly chosen areas containing more than 200 Iba1 or LAMP-2 positive cells under fluorescence microscope as the total cell numbers. When stained with anti-Iba1 antibody, the numbers of microglia containing engulfed fAβ_{42} were determined by counting cells with Alexa 594 internalization around nuclei other than on the cell surface. When stained with anti-LAMP-2 antibody, the numbers of microglia containing engulfed fAβ_{42} were determined by counting cells with the colocalization of Alexa 488 and Alexa 594 fluorescence. The percentages of fAβ_{42}-phagocytosed microglia pre-treated with different concentrations of JTT were shown as means and standard deviation (S.D.) from three independent experiments with Iba1 and 4G8 staining and one experiment with LAMP-2 and 4G8 staining. While the percentages of fAβ_{42}-phagocytosed microglia pre-treated with 200 μg/ml JTT for different time periods were shown as means and SD from three independent experiments with Iba1 and 4G8 staining. The percentages of fAβ_{42}-phagocytosed BMM were analyzed similarly from four mice per group with Iba1 and 4G8 staining.

Nitric oxide (NO) quantification

The Griess reaction is extensively used as an indicator of NO production by cultured cells. Primary microglia were plated on 48-well culture plates at 1×10^5 cells/well, and treated with or without 200 μg/ml JTT for 24 hrs. Afterwards, the culture medium was changed with or without 10 μM fAβ_{42} for another 24 hrs incubation. The media collected were centrifuged and the cell-free supernatants were then quantitatively determined for total NO production using a total NO assay kit (Endogen, Pierce Biotechnology, Rockford, IL, USA). The assay was carried out according to the manufacturer's protocol.

Statistical analyses

All results were expressed as means ± S.D. The statistical significance of differences was determined by two-tailed Student's *t*-test or analysis of variance (ANOVA) followed by the post-hoc multiple comparison.

Results

Effects of JTT on the morphological change of microglial activation

The effect of JTT on microglial activation was first revealed by observing prominent morphological changes of primary microglia treated with JTT under the phase contrast microscope. It

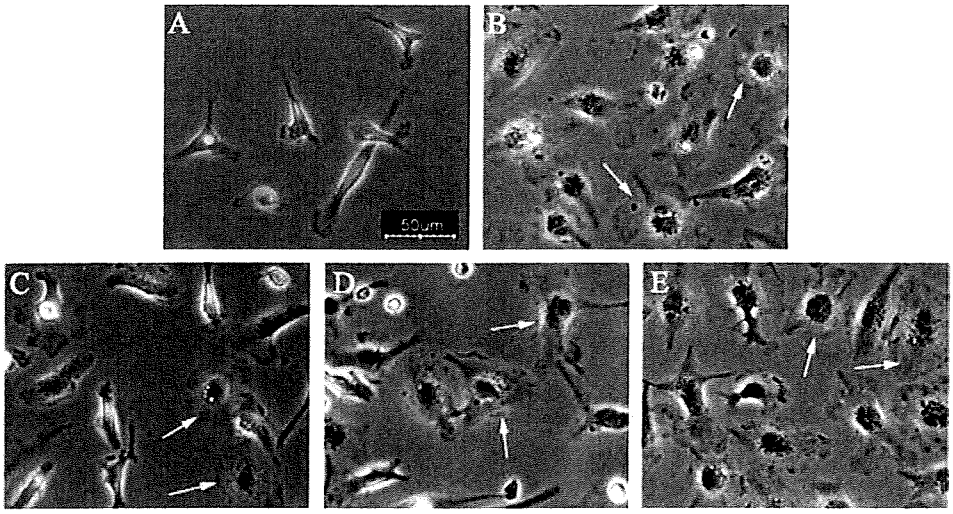

Fig. 1. JTT changed the morphological appearance of primary microglia. Primary microglia were cultured for 24 hrs in (A) unstimulated condition, (B) LPS (0.1 μg/ml), (C) JTT (100 μg/ml), (D) JTT (200 μg/ml), and (E) JTT (400 μg/ml) and observed under the phase contrast microscope. The arrows show some of the activated microglia with amoeboid morphology. Scale bar, 50 μm.

is well known that resting microglia adopt a characteristic highly ramified and elongated morphological appearance with small cell bodies, while activated microglia undergo dramatic morphological changes showing amoeboid morphology with large cell bodies and short processes (Kreutzberg 1996). When we treated primary microglia with different concentrations of JTT or LPS for 24 hrs, we observed that they showed obvious activated morphological appearance, particularly in 200 and 400 μg/ml JTT-treated groups (Fig. 1).

Effect of JTT on microglial proliferation and viability

To investigate the possible role of JTT in the proliferation and activation of microglia, next we examined whether JTT could sustain the cell proliferation of primary microglia by the WST-1 assay. As expected, JTT increased microglial proliferation and viability in a slightly dose-dependent fashion. Compared with LPS, JTT showed similar or more promoting effects on microglial proliferation and viability (Fig. 2). From this result and the above morphological change result, we chose the concentrations of 200 and 400 μg/ml for some of the following experiments.

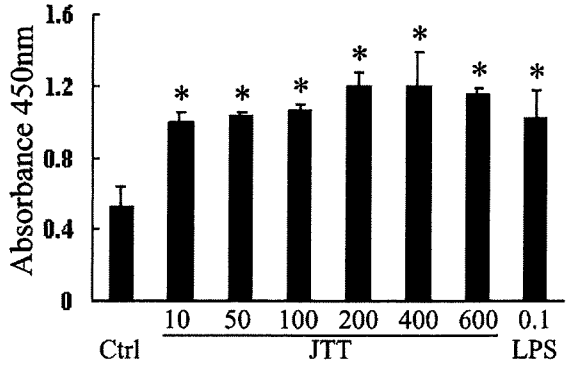

Fig. 2. JTT induced cell proliferation of primary microglia by the WST-1 cell proliferation assay. Primary microglia were seeded at a density of 2×10^4 cells/well in a 96-well microtiter plate as described in the Materials and Methods. After treatment with different concentrations of JTT as well as LPS as a positive control for 48 hrs, the cultures were added with the WST-1 reagent followed by 4 hrs incubation, and then the absorbance at 450 nm was measured. Mean ± S.D. values from a single experiment were obtained in triplicate. Similar results were obtained in two separate experiments. $*p < 0.01$ vs control group (unstimulated condition) analyzed by Dunnett's test in ANOVA.

Effect of JTT on the surface expression of CD11b

The flow cytometric assay was used to check the expression of surface marker CD11b on microglial cell line Ra2, which indicates the activation of microglia. Ra2 cells have been confirmed to have similar properties to primary microglia, and have been generally used as the substitutes of primary microglia in experimental research (Ito et al. 2005, 2006; Laquintana et al. 2007; Roepstorff et al. 2007). Ra2 cells were used in the flow cytometric assay because they showed easily-detached property after treatment than primary microglia. So Ra2 cells were more suitable for this assay in order to obtain more creditable results. Two peaks were obtained apparently in every treated group but not in an unstimulated condition after either 24 or 48 hrs treatment, indicating that the latter peak should be formed by activated cells (M1). After 24 hrs treatment with JTT or LPS, the percentage of activated cell number and their mean fluorescence intensity (mFI) were both increased compared to the negative control group, but there was no significant difference (data not shown). However, after 48 hrs treatment, there was significant difference when the above two indexes were analyzed, while there was no difference between the 200 and 400 μg/ml JTT treatment groups (Fig. 3). JTT increased the cell number percentage and mFI of M1 by about 50% and 170%, respectively, relative to the negative control. These results

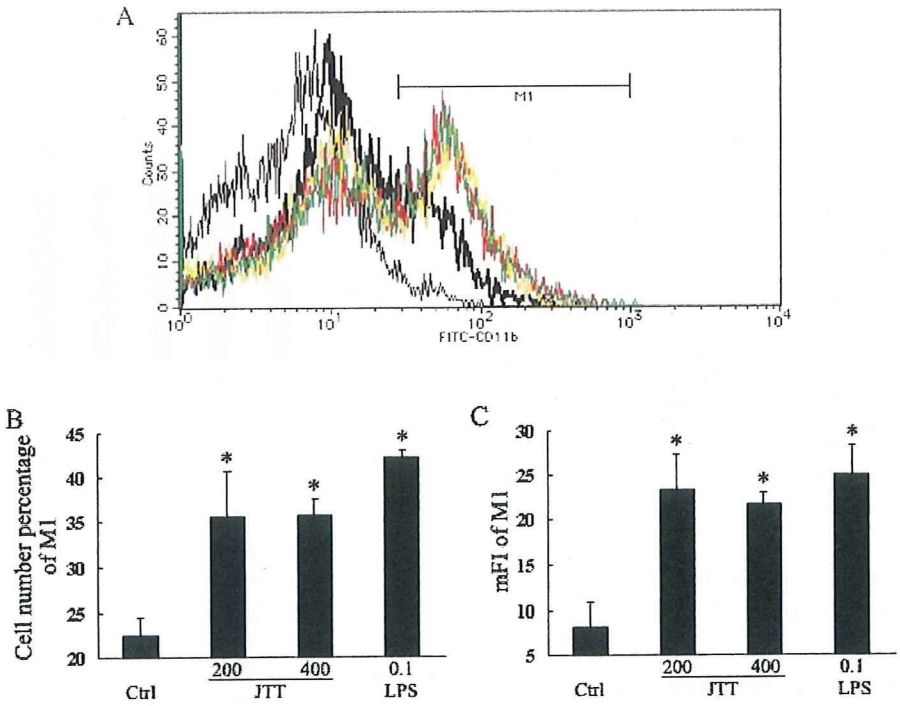

Fig. 3. JTT increased the surface expression of CD11b. Ra2 microglial cells were treated with 200, 400 μg/ml JTT or 0.1 μg/ml LPS for 48 hrs as described in the Materials and Methods. After gently detached, Ra2 cells were stained with FITC-conjugated anti-CD11b antibody for the FACS analysis. (A) Overlay of flow cytometry histograms of untreated cells without staining (gray line), untreated cells as control (black line), 200 μg/ml JTT-treated cells (red line), 400 μg/ml JTT-treated cells (yellow line) and LPS-treated cells (green line). M1, which referred to the second peak, represents the activated cells whose CD11b expression was increased. (B) The cell number percentage of M1 in each group. (C) Mean fluorescence intensity of M1 in each group. Mean ± S.D. values from a single experiment were performed in triplicate. Similar results were obtained in two independent experiments. *$p < 0.01$ vs control group analyzed by Dunnett's test in ANOVA.

confirmed that JTT could induce the surface expression of an activation marker CD11b on microglia, but it might take at least 48 hrs to show this effect.

Effect of JTT on Microglial Phagocytosis of $fA\beta_{42}$

Since the above findings confirmed that JTT could induce the proliferation and activation of microglia, we next examined whether JTT could enhance microglial phagocytosis of $fA\beta_{42}$. We could see that JTT did enhance the microglial phagocytosis of $fA\beta_{42}$ obviously after 24 hrs treatment when the concentration of JTT was higher than 200 μg/ml, but did not show a concentration-dependent fashion (Fig. 4E). The 200 μg/ml JTT-treated group got the highest percentage of phagocytosed cells of 60.5 ± 5.4%, which is higher than the negative control (33.7 ± 4.4%) and the LPS positive control (46.9 ± 2.3%) by 26.8 ± 1.3% and 13.6 ± 6.2%, respectively. To examine whether the effect of JTT showed time-dependent fashion, 200 μg/ml JTT was used to treat primary microglia for different time periods. The 24 hrs treatment group showed the highest percentage of phagocytosed cells of 60.4 ± 4.4%. No evident time-dependent fashion was seen as shown in Fig. 4F.

Effect of JTT on BMM phagocytosis of $fA\beta_{42}$

The $fA\beta_{42}$ phagocytosis was also investigated in BMM in this study. The BMM from the two groups (four mice each) which had been pre-administrated with or without JTT were cultured for 12 - 13 days as described above, and then their ability of $fA\beta_{42}$ phagocytosis was examined using

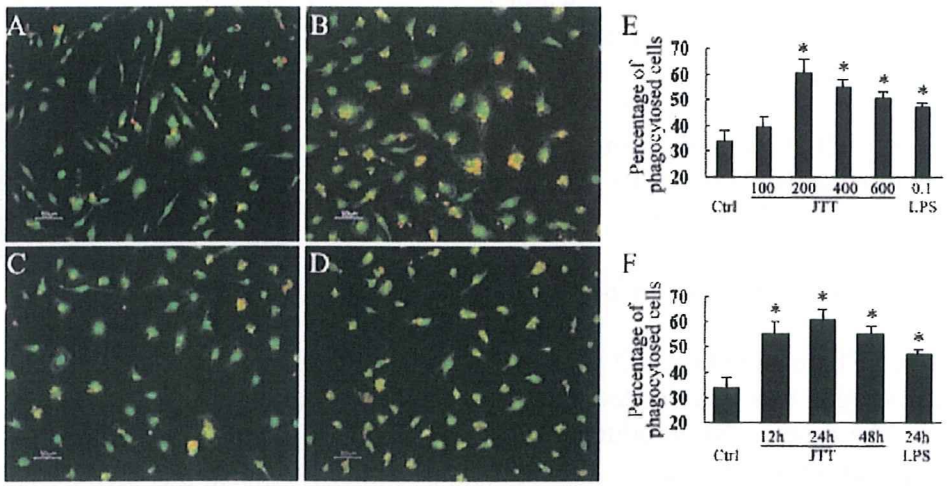

Fig. 4. JTT enhanced the phagocytosis of $fA\beta_{42}$ in primary microglia. Primary microglia were treated with JTT or LPS. Then the culture medium was changed and 1 μM $fA\beta_{42}$ was added for further 3 hrs incubation followed by immunofluorescence double staining as described in the Materials and Methods. (A-D) The cells were stained with antibodies directed against Iba1 and 4G8, and then with Alexa 488 (green) and Alexa 594 (red)-conjugated secondary antibodies, respectively. Under fluorescence microscope, colocalization of microglia and $fA\beta_{42}$ was shown by yellow color as a result of superimposing fluorescence images of microglia (green) and $fA\beta_{42}$ (red). (A) Control (unstimulated condition, 24 hrs). (B) JTT (200 μg/ml, 24 hrs). (C) JTT (400 μg/ml, 24 hrs). (D) LPS (0.1 μg/ml, 24 hrs). (E) Microglia were treated with different concentrations of JTT or LPS for 24 hrs. Percentages of phagocytosed cells were counted. Mean ± S.D. values were obtained from three separate experiments with Iba1 and 4G8 staining and one experiment with LAMP-2 and 4G8 staining (figure not shown). (F) Microglia were treated with 200 μg/ml JTT for distinct time periods (12, 24, 48 hrs) or 0.1 μg/ml LPS for 24 hrs. Percentages of phagocytosed cells were counted (figure not shown). Mean ± S.D. values were obtained from three separate experiments with Iba1 and 4G8 staining. Scale bars represent 50 μm. *$p < 0.01$ vs control group analyzed by Dunnett's test in ANOVA.

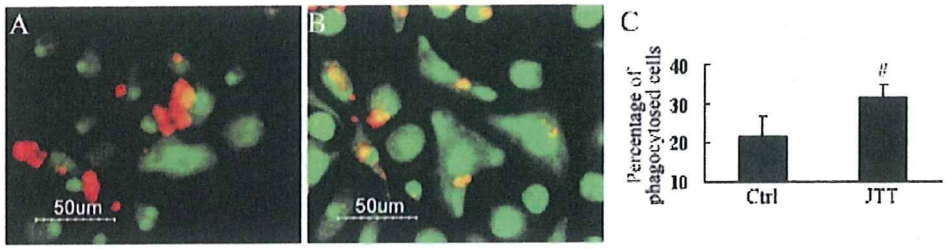

Fig. 5. JTT enhanced the phagocytosis of fAβ_{42} in BMM. BMM were obtained from mice with or without JTT administration and cultured for about 2 weeks. Then the culture medium was changed and 1 μM fAβ_{42} was added for further 3 hrs incubation followed by immunofluorescence double staining as described in the Materials and Methods. (A-B) The cells were stained with antibodies directed against Iba1 and 4G8, and then with Alexa 488 (green) and Alexa 594 (red)-conjugated secondary antibodies, respectively. Under fluorescence microscope, colocalization of BMM and fAβ_{42} was shown by yellow color as a result of superimposing fluorescence images of BMM (green) and fAβ_{42} (red). (A) Control group (without JTT administration), (B) JTT administration group, (C) Percentages of phagocytosed cells. Mean ± S.D. values were obtained from four mice. Scale bars represent 50 μm. #$p < 0.05$ vs control group analyzed by two-tailed Student's t test.

immunofluorescence double staining according to the same protocol mentioned above. As shown in Fig. 5, some BMM from JTT-administrated mice showed larger cell bodies and stronger signal of Iba1 staining (Fig. 5B) compared to the control group (Fig. 5A), as well as the higher percentage of fAβ_{42}-phagocytosed cells (31.6 ± 3.3% vs 21.6 ± 5.2%, respectively, $p < 0.05$) (Fig. 5C).

Effect of JTT on NO production in primary microglia

The effect of JTT treatment on NO production in primary microglia was investigated by the Griess reaction. The ratio of NO production to the control group was shown in Fig. 6. Twenty hundred μg/ml JTT was used to treat primary microglia. It slightly increased NO production but no statistical difference compared to the control group ($p = 0.396$), but LPS or 10 μM fAβ_{42} did increase ($p = 0.000$ and 0.008, respectively). And between the JTT and LPS groups, there was also significant difference ($p = 0.002$). In the presence of 10 μM fAβ_{42}, although JTT treatment did not reduce the NO production, at least it did not increase the NO production ($p = 0.396$).

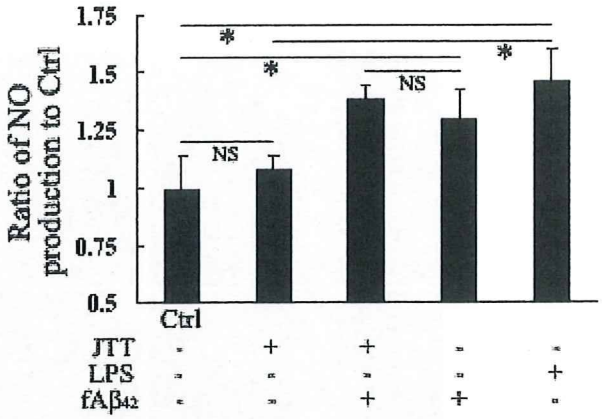

Fig. 6. JTT did not increase the production of NO in primary microglia. Primary microglia were treated with 200 μg/ml JTT or 0.1 μg/ml LPS for the first 24 hrs, then the culture was continued with or without 10 μM fAβ_{42} for another 24 hrs. The supernatants were obtained and their contents of NO were measured by the Griess reaction as described in the Materials and Methods. The ratios of NO production of each group to the control group (untreated condition) were shown. Mean ± S.D. values were obtained from a single experiment in triplicate. Similar results were obtained in two separate experiments. *$p < 0.01$ analyzed by least significant difference test in ANOVA. NS, not significant.

Discussion

Microglia represent the brain innate immune system and hence the first line of defense against

invading pathogens and serve as specialized sensors for brain tissue injury (Streit et al. 2005; Conde and Streit 2006). Under pathological situations, such as neurodegenerative disease, microglia become activated, migrate to and surround damaged or dead cells, and subsequently clear cellular debris from the area, similar to the phagocytic active macrophages of the peripheral immune system (Fetler and Amigorena 2005). At the same time, activated microglia are also revealed to produce NO and some kinds of pro-inflammatory cytokines, which are considered to enhance the inflammation and exacerbate the diseases. There is considerable debate as to whether activated microglia are beneficial or harmful in AD. This may, however depend on the degree of activation. Nowadays, many researchers focused on how to inhibit microglial activation to restrain the inflammation. But it should also be noted that activated microglia are able to reduce Aβ accumulation by increasing its phagocytosis, clearance and degradation (Frautschy et al. 1998; Qiu et al. 1998; Yan et al. 2003). While an exaggerated immune response can certainly be detrimental to the CNS, increasing evidence demonstrates that a controlled inflammatory reaction in the brain can be greatly beneficial to the health and proper function of the CNS. So in the present study, we attempted to search a way through which we can make a controlled activation of microglia.

Among more than one hundred kinds of herbal medicines, JTT is well known to enhance the immunological functions (Matsumoto et al. 2000). Nowadays, since its anti-cancer effects (Dai et al. 2001; Tagami et al. 2004) and suppressive effects on toxicity of anti-cancer drugs (Sugiyama et al. 1995a, b) were confirmed, JTT is often clinically used for the treatment of cancer patients. And JTT has also been demonstrated to have influence not only on the acquired immune system but also the innate immune response related with macrophages (Chino et al. 2005). In the neurological diseases, AD has been demonstrated to be highly related with immune response and inflammation. Preliminary results from in vivo experiment in our laboratory supported that JTT administration diminished the senile plaques in AD transgenic mouse (Hara et al. unpublished observation). These findings prompted us to clarify the possible mechanism of the diminishing of senile plaques in order to search a new possible therapeutic way for AD.

First, we treated naive primary microglia with different concentrations of JTT, a dramatic morphological change from resting ramified cells to amoeboid microglia was observed, as well as decreased refraction and better adherent property, obviously in 200 and 400 μg/ml groups. This finding encouraged us to detect whether JTT activated microglia definitely.

Then the fact that JTT did activate microglia was demonstrated by the WST-1 cell proliferation assay and flow cytometric assay to check the surface expression of an activation marker CD11b. From the cell proliferation assay, JTT increased microglial proliferation and viability even though at a low concentration (10 μg/ml) with a slight concentration-dependent fashion. In the flow cytometric analysis, CD11b, a well-known activation marker of microglia/macrophages, was used. As expected, two peaks appeared obviously, similar with the LPS-treated group, indicating that the second peak represented the activated cells. These findings revealed that the Kampo formulation JTT could induce microglial proliferation and activation.

Then, important in our experiment was the phagocytosis-enhancing effect of JTT. There are very limited reports about phagocytosis-enhancing effects using crude extracts or oral administration of herbal medicine. According to the previous report (Liu et al. 2005), phagocytosis might be dissociated from inflammatory microglial activation in relation to the AD stage. So in the fAβ_{42}-phagocytosis assay, we chose a low (1 μM) fAβ_{42} concentration. Although 100 μg/ml JTT induced microglial proliferation, it showed no significant effect on fAβ_{42}-phagocytosis (p = 0.171); while 200 μg/ml JTT treatment increased the percentage of phagocytosed cells by about 80% compared to the unstimulated group, indicating that to show phagocytosis-enhancing effect, a relatively higher concentration was needed than to induce microglial proliferation. This concen-

tration of 200 μg/ml in in vitro experiments was consistent with the dosage for human use and the previous reports about the in vitro studies of JTT (Hisha et al. 1997; Kamiyama et al. 2005). Although 12 hrs treatment was enough to enhance the phagocytosis, no time-dependent fashion was detected. In recent studies, more attention was paid on the effect of bone marrow-derived microglia on restricting senile plaque formation (Malm et al. 2005; Simard et al. 2006). In this study, using M-CSF, we induced the bone marrow stem cells or myeloid progenitor cells to differentiate to macrophages, and we found that orally administrated JTT could also enhance the phagocytosis of fAβ_{42} in BMM. However, we used a dose of 100 mg/ml according to our previous protocol. As mentioned above, this is much higher than the dosage for human use. Although animals were tolerated well with the dose, we need to repeat the experiment with lower doses.

Activated microglia can produce NO and other pro-inflammatory cytokines, most of which are considered to be detrimental to neurons, and play an important role in the pathogenesis of AD. Excessive production of NO can mediate oxidative stress as well as amplify inflammation cascade reactions. Here we examined the NO production as a representative index. In this assay, a relatively higher (10 μM) fAβ_{42} concentration was used. First, JTT treatment did not increase the NO production, but LPS and fAβ_{42} did. Second, in the presence of fAβ_{42}, although JTT pre-treatment did not reduce the NO production, at least it did not increase NO. This finding and the above results indicated that with proper concentrations and time periods of treatment, JTT might induce activation and mediate phagocytosis without eliciting excessive production of neurotoxic NO in microglia/macrophages.

In summary, the results of this study demonstrated that Kampo formulation JTT could induce microglial proliferation and activation, and also enhance fAβ_{42}-phagocytosis in microglia and BMM without excessive NO production. To our knowledge, this is the first report indicating that JTT has enhancing effect of fAβ_{42}-phagocytosis on microglia/macrophages. These findings support our previous finding that JTT administration diminished the senile plaque in AD transgenic mouse, which might be due to the enhanced phagocytosis of Aβ by microglia, and the phagocytosis-enhancing effect of JTT might not be accompanied by excessive inflammatoty mediators' production. This is also consistent with the previous reports showing the anti-inflammatory and anti-oxidative activities of the components of JTT (Lee et al. 2003; Matsui et al. 2004). These findings suggest that JTT administration would be a potential therapeutic or preventive approach for AD. Further intensive study should be performed in order to evaluate its therapeutic effect by in vivo study and to elucidate the underline mechanism in detail.

Acknowledgments

This study was partially supported by Grant-in-Aid for Scientific Research on Priority Areas (17025056) from the Ministry of Education, Culture, Sports, Science and Technology. Huayan Liu is a fellow supported by Sasakawa Foundation. We thank Sasakawa Memorial Health Foundation and Japan China Medical Association for their kind support. We also thank Dr. A. Suzumura, M. Sawada, K. Takahashi, H. Wakita, A. Watanabe, S. Kataoka, K. Adachi, K. Yoshizaki, and K. Takeda for their kind help and discussion in this work.

References

Bae, E.A., Kim, E.J., Park, J.S., Kim, H.S., Ryu, J.H. & Kim, D.H. (2006) Ginsenosides Rg3 and Rh2 inhibit the activation of AP-1 and protein kinase A pathway in lipopolysaccharide/ interferon-γ-stimulated BV-2 microglial cells. *Planta. Med.*, **72**, 627-633.

Baltina, L.A. (2003) Chemical modification of glycyrrhizic acid as a route to new bioactive compounds for medicine. *Curr. Med. Chem.*, **10**, 155-171.

Chino, A., Sakurai, H., Choo, M.K., Koizumi, K., Shimada, Y., Terasawa, K. & Saiki, I. (2005) Juzentaihoto, a Kampo medicine, enhances IL-12 production by modulating Toll-like receptor 4 signaling pathways in murine peritoneal exudate macrophages. *Int. Immunopharmacol.*, **5**, 871-882.

Conde, J.R. & Streit, W.J. (2006) Microglia in the aging brain. *J. Neuropathol. Exp. Neurol.*, **65**, 199-203.

Cuadros, M.A. & Navascues, J. (1998) The origin and differentiation of microglial cells during development. *Prog. Neurobiol.*, **56**, 173-189.

Dai, Y., Kato, M., Takeda, K., Kawamoto, Y., Akhand, A.A., Hossain, K., Suzuki, H. & Nakashima, I. (2001) T-cell-immunity-based inhibitory effects of orally administered herbal medicine juzen-taiho-to on the growth of primarily developed melanocytic tumors in RET-transgenic mice. *J. Invest. Dermatol.*, **117**, 694-701.

Dhuley, J.N. (1999) Anti-oxidant effects of cinnamon (Cinnamomum verum) bark and greater cardamom (Amomum subulatum) seeds in rats fed high fat diet. *Indian. J. Exp. Biol.*, **37**, 238-242.

Fetler, L. & Amigorena, S. (2005) Neuroscience. Brain under surveillance: the microglia patrol. *Science*, **309**, 392-393.

Frautschy, S.A., Yang, F., Irrizarry, M., Hyman, B., Saido, T.C., Hsiao, K. & Cole, G.M. (1998) Microglial response to amyloid plaques in APPsw transgenic mice. *Am. J. Pathol.*, **152**, 307-317.

Hisha, H., Yamada, H., Sakurai, M.H., Kiyohara, H., Li, Y., Yu, C., Takemoto, N., Kawamura, H., Yamaura, K., Shinohara, S., Komatsu, Y., Aburada, M. & Ikehara, S. (1997) Isolation and identification of hematopoietic stem cell-stimulating substances from Kampo (Japanese herbal) medicine, Juzen-taiho-to. *Blood*, **90**, 1022-1030.

Ito, S., Sawada, M., Haneda, M., Fujii, S., Oh-Hashi, K., Kiuchi, K., Takahashi, M. & Isobe, K. (2005) Amyloid-β peptides induce cell proliferation and macrophage colony-stimulating factor expression via the PI3-kinase/Akt pathway in cultured Ra2 microglial cells. *FEBS. Lett.*, **579**, 1995-2000.

Ito, S., Sawada, M., Haneda, M., Ishida, Y. & Isobe, K. (2006) Amyloid-beta peptides induce several chemokine mRNA expressions in the primary microglia and Ra2 cell line via the PI3K/Akt and/or ERK pathway. *Neurosci. Res.*, **56**, 294-299.

Kamiyama, H., Takano, S., Ishikawa, E., Tsuboi, K. & Matsumura, A. (2005) Anti-angiogenic and immunomodulatory effect of the herbal medicine "Juzen-taiho-to" on malignant glioma. *Biol. Pharm. Bull.*, **28**, 2111-2116.

Keum, Y.S., Han, S.S., Chun, K.S., Park, K.K., Park, J.H., Lee, S.K. & Surh, Y.J. (2003) Inhibitory effects of the ginsenoside Rg3 on phorbol ester-induced cyclooxygenase-2 expression, NF-κB activation and tumor promotion. *Mutat. Res.*, **523-524**, 75-85.

Kopec, K.K. & Carroll, R.T. (1998) Alzheimer's β-amyloid peptide 1-42 induces a phagocytic response in murine microglia. *J. Neurochem.*, **71**, 2123-2131.

Kreutzberg, G.W. (1996) Microglia: a sensor for pathological events in the CNS. *Trends. Neurosci.*, **19**, 312-318.

Laquintana, V., Denora, N., Lopedota, A., Suzuki, H., Sawada, M., Serra, M., Biggio, G., Latrofa, A., Trapani, G. & Liso, G. (2007) *N*-Benzyl-2-(6,8-dichloro-2-(4-chlorophenyl) imidazo [1,2-*a*] pyridin-3-yl)-*N*-(6-(7-nitrobenzo [*c*] [1,2,5] oxadiazol-4-ylamino) hexyl) acetamide as a new fluorescent probe for peripheral benzodiazepine receptor and microglial cell visualization. *Bioconjug. Chem.*, **18**, 1397-1407.

Lee, S.J., Lee, I.S. & Mar, W. (2003) Inhibition of inducible nitric oxide synthase and cyclooxygenase-2 activity by 1,2,3,4,6-penta-O-galloyl-beta-D-glucose in murine macrophage cells. *Arch. Pharm. Res.*, **26**, 832-839.

Liu, Y., Walter, S., Stagi, M., Cherny, D., Letiembre, M., Schulz-Schaeffer, W., Heine, H., Penke, B., Neumann, H. & Fassbender, K. (2005) LPS receptor (CD14): a receptor for phagocytosis of Alzheimer's amyloid peptide. *Brain*, **128**, 1778-1789.

Malm, T.M., Koistinaho, M., Parepalo, M., Vatanen, T., Ooka, A., Karlsson, S. & Koistinaho, J. (2005) Bone-marrow-derived cells contribute to the recruitment of microglial cells in response to β-amyloid deposition in APP/PS1 double transgenic Alzheimer mice. *Neurobiol. Dis.*, **18**, 134-142.

Matsui, S., Matsumoto, H., Sonoda, Y., Ando, K., Aizu-Yokota, E., Sato, T. & Kasahara, T. (2004) Glycyrrhizin and related compounds down-regulate production of inflammatory chemokines IL-8 and eotaxin 1 in a human lung fibroblast cell line. *Int. Immunopharmacol.*, **4**, 1633-1644.

Matsumoto, T., Sakurai, M.H., Kiyohara, H. & Yamada, H. (2000) Orally administered decoction of Kampo (Japanese herbal) medicine, "Juzen-Taiho-To" modulates cytokine secretion and induces NKT cells in mouse liver. *Immunopharmacology*, **46**, 149-161.

Park, E.K., Choo, M.K., Han, M.J. & Kim, D.H. (2004) Ginsenoside Rh1 possesses antiallergic and anti-inflammatory activities. *Int. Arch. Allergy. Immunol.*, **133**, 113-120.

Qiu, W.Q., Walsh, D.M., Ye, Z., Vekrellis, K., Zhang, J., Podlisny, M.B., Rosner, M.R., Safavi, A., Hersh, L.B. & Selkoe, D.J. (1998) Insulin-degrading enzyme regulates extracellular levels of amyloid beta-protein by degradation. *J. Biol. Chem.*, **273**, 32730-32738.

Raine, C.S. (1994) Multiple sclerosis: immune system molecule expression in the central nervous system. *J. Neuropathol. Exp. Neurol.*, **53**, 328-337.

Roepstorff, K., Rasmussen, I., Sawada, M., Cudre-Maroux, C., Salmon, P., Bokoch, G., van Deurs, B. & Vilhardt, F. (2007) Stimulus dependent regulation of the phagocyte NADPH oxidase by a VAV1, rac1, and PAK1 signaling axis. *J. Biol. Chem.*, Epub ahead of print.

Rogers, J., Luber-Narod, J., Styren, S.D. & Civin, W.H. (1988) Expression of immune system-associated antigens by cells of the human central nervous system: relationship to the pathology of Alzheimer's disease. *Neurobiol. Aging*, **9**, 339-349.

Sawada, M., Imai, F., Suzuki, H., Hayakawa, M., Kanno, T. & Nagatsu, T. (1998) Brain-specific gene expression by immortalized microglial cell-mediated gene transfer in the mammalian brain. *FEBS. Lett.*, **433**, 37-40.

Shon, Y.H. & Nam, K.S. (2003) Protective effect of Astragali radix extract on interleukin 1β-induced inflammation in human amnion. *Phytother. Res.*, **17**, 1016-1020.

Simard, A.R., Soulet, D., Gowing, G., Julien, J.P. & Rivest, S. (2006) Bone marrow-derived microglia play a critical role in restricting senile plaque formation in Alzheimer's disease. *Neuron.*, **49**, 489-502.

Streit, W.J., Conde, J.R., Fendrick, S.E., Flanary, B.E. & Mariani, C.L. (2005) Role of microglia in the central nervous system's immune response. *Neurol. Res.*, **27**, 685-691.

Sugiyama, K., Ueda, H. & Ichio, Y. (1995a) Protective effect of juzen-taiho-to against carboplatin-induced toxic side effects in mice. *Biol. Pharm. Bull.*, **18**, 544-548.

Sugiyama, K., Ueda, H., Ichio, Y. & Yokota, M. (1995b) Improvement of cisplatin toxicity and lethality by juzen-taiho-to in mice. *Biol. Pharm. Bull.*, **18**, 53-58.

Suzumura, A., Mezitis, S.G., Gonatas, N.K. & Silberberg, D.H. (1987) MHC antigen expression on bulk isolated macrophage-microglia from newborn mouse brain: induction of Ia antigen expression by gamma-interferon. *J. Neuroimmunol.*, **15**, 263-278.

Tagami, K., Niwa, K., Lian, Z., Gao, J., Mori, H. & Tamaya, T. (2004) Preventive effect of Juzen-taiho-to on endometrial carcinogenesis in mice is based on Shimotsu-to constituent. *Biol. Pharm. Bull.*, **27**, 156-161.

Takahashi, K., Prinz, M., Stagi, M., Chechneva, Olga. & Neumann, H. (2007) TREM2- transduced myeloid precursors mediate nervous tissue debris clearance and facilitate recovery in an animal model of multiple sclerosis. *PLoS. Med.*, **4**, e124.

Wang, P., Zhang, Z., Ma, X., Huang, Y., Liu, X., Tu, P. & Tong, T. (2003) HDTIC-1 and HDTIC-2, two compounds extracted from Astragali Radix, delay replicative senescence of human diploid fibroblasts. *Mech. Ageing Dev.*, **124**, 1025-1034.

Weldon, D.T., Rogers, S.D., Ghilardi, J.R., Finke, M.P., Cleary, J.P., O'Hare, E., Esler, W.P., Maggio, J.E. & Mantyh, P.W. (1998) Fibrillar β-amyloid induces microglial phagocytosis, expression of inducible nitric oxide synthase, and loss of a select population of neurons in the rat CNS in vivo. *J. Neurosci.*, **18**, 2161-2173.

Yan, Q., Zhang, J., Liu, H., Babu-Khan, S., Vassar, R., Biere, A.L., Citron, M. & Landreth, G. (2003) Anti-inflammatory drug therapy alters beta-amyloid processing and deposition in an animal model of Alzheimer's disease. *J. Neurosci.*, **23**, 7504-7509.

Journal of Controlled Release 142 (2010) 431–437

Contents lists available at ScienceDirect

Journal of Controlled Release

journal homepage: www.elsevier.com/locate/jconrel

Prevention of hepatic ischemia–reperfusion injury by pre-administration of catalase-expressing adenovirus vectors

Masahiro Ushitora [a,b], Fuminori Sakurai [a,*], Tomoko Yamaguchi [a,c], Shin-ichiro Nakamura [d], Masuo Kondoh [b], Kiyohito Yagi [b], Kenji Kawabata [a], Hiroyuki Mizuguchi [a,c,*]

[a] Laboratory of Gene Transfer and Regulation, National Institute of Biomedical Innovation, Osaka, Japan
[b] Laboratory of Bio-Functional Molecular Chemistry, Graduate School of Pharmaceutical Sciences, Osaka University, Osaka, Japan
[c] Department of Biochemistry and Molecular Biology, Graduate School of Pharmaceutical Sciences, Osaka University, Osaka, Japan
[d] Research Center of Animal Life Science, Shiga University of Medical Science, Otsu-City, Shiga, Japan

ARTICLE INFO

Article history:
Received 17 August 2009
Accepted 25 November 2009
Available online 29 November 2009

Keywords:
Adenovirus vector
Reactive oxygen
Ischemia/reperfusion
Liver
Catalase
Hepatectomy

ABSTRACT

Liver ischemia/reperfusion (I/R) injury, which is mainly caused by the generation of reactive oxygen species (ROS) during the reperfusion, remains an important clinical problem associated with liver transplantation and major liver surgery. Therefore, ROS should be detoxified to prevent hepatic I/R-induced injury. Delivery of antioxidant genes into liver is considered to be promising for prevention of hepatic I/R injury; however, therapeutic effects of antioxidant gene transfer to the liver have not been fully examined. The aim of this study was to examine whether adenovirus (Ad) vector-mediated catalase gene transfer in the liver is an effective approach for scavenging ROS and preventing hepatic I/R injury. Intravenous administration of Ad vectors expressing catalase, which is an antioxidant enzyme scavenging H_2O_2, resulted in a significant increase in catalase activity in the liver. Pre-injection of catalase-expressing Ad vectors dramatically prevented I/R-induced elevation in serum alanine aminotransferase (ALT) and aspartate aminotransferase (AST) levels, and hepatic necrosis. The livers were also protected in another liver injury model, CCl_4-induced liver injury, by catalase-expressing Ad vectors. Furthermore, the survival rates of mice subjected to both partial hepatectomy and I/R treatment were improved by pre-injection of catalase-expressing Ad vectors. On the other hand, control Ad vectors expressing β-galactosidase did not show any significant preventive effects in the liver on the models of I/R-induced or CCl_4-induced hepatic injury described above. These results indicate that hepatic delivery of the catalase gene by Ad vectors is a promising approach for the prevention of oxidative stress-induced liver injury.

1. Introduction

Hepatic ischemia/reperfusion (I/R) injury occurs in a variety of clinical settings, such as in liver transplantation, hepatic failure after shock, and liver surgery, and results in severe damages that substantially contribute to the morbidity and mortality of such cases [1–3]. Hepatic I/R injury is caused by reactive oxygen species (ROS), including superoxide anion, hydrogen oxide, and hydroxyl radical, which are generated by reperfusion of the ischemic tissue. ROS induce lipid peroxidation and damages to proteins and nucleic acids, leading to parenchymal cell dysfunction and necrosis, increased vascular permeability, and inflammatory cell infiltration [4]. Therefore, ROS should be detoxified to prevent hepatic I/R injury.

In previous animal studies, antioxidative enzyme catalase and superoxide dismutase (SOD) were systemically administered to neutralize ROS and prevent I/R-induced hepatic injury. Although catalase and SOD are endogenously expressed in the cells, the expression levels of these enzymes are insufficient to prevent I/R injury. Administration of antioxidant enzymes exhibited therapeutic effects on ROS-induced diseases, including I/R-induced hepatic injury, in several studies [5–8]; however, these enzymes are known to be rapidly eliminated from the circulation following systemic administration, which limits their therapeutic potential, [9,10] although chemical modification of antioxidant enzymes has been carried out to enhance their plasma half-lives and tissue accessibility [5,6,9]. In addition, systemically administered antioxidant enzymes might be degraded in the endosomes/lysosomes because they are internalized into the cells via the endocytosis pathway.

The delivery of therapeutic genes encoding antioxidant enzymes into the liver is considered to be a promising strategy to overcome these problems. Previous studies have demonstrated that ROS-mediated injury was efficiently prevented by over-expression of antioxidant

* Corresponding authors. Sakurai is to be contacted at Laboratory of Gene Transfer and Regulation, National Institute of Biomedical Innovation, 5-6-7 Saito Asagi, Ibaraki, Osaka, 567-0085, Japan. Tel.: +81 72 641 9815; fax: +81 72 641 9816. Mizuguchi, Department of Biochemistry and Molecular Biology, Graduate School of Pharmaceutical Sciences, Osaka University, 1-6 Yamadaoka, Suita, Osaka, 565-0871, Japan. Tel./fax: +81 6 6879 8185.
E-mail addresses: sakurai@nibio.go.jp (F. Sakurai), mizuguch@phs.osaka-u.ac.jp (H. Mizuguchi).

0168-3659/$ – see front matter.
doi:10.1016/j.jconrel.2009.11.024

enzymes in various tissues, including the artery, pancreatic islets, and brain [11–13]. A variety of types of gene delivery vehicles have been employed for delivery of antioxidative genes so far, and replication-incompetent adenovirus (Ad) vectors have several advantages over other vehicles to deliver antioxidant genes to the liver. First, Ad vectors have high tropism to livers. A more than 10^3-fold higher transgene expression is found in the liver, compared with other organs, following systemic administration [14–16]. Second, non-dividing cells are efficiently transduced with Ad vectors. Hepatocytes do not actively divide under normal conditions. Non-viral gene delivery vehicles have been used for prevention of hepatic I/R injury in previous studies [17,18]; however, non-viral gene delivery vehicles mediate inefficient transfection in non-dividing cells. Third, the Ad vector genome is not integrated into the host genome, indicating that transduction with Ad vectors is unlikely to induce insertional mutagenesis in hepatocytes. Fourth, Ad vector-mediated gene expression in liver persists for 1–2 weeks, [19,20] in contrast, rapid reduction in plasmid DNA-mediated transgene expression in organs is found after injection of non-viral gene delivery vehicles [21,22]. In spite of these advantages of Ad vectors, the ability of Ad vectors expressing antioxidant enzymes to prevent hepatic I/R injury has not been fully examined probably because Ad vectors are generally considered more toxic than non-viral gene delivery vehicles; however, our group demonstrated that intravenous administration of Ad vectors induces less amounts of inflammatory cytokines than cationic lipid/plasmid DNA complexes [23]. In addition, fiber-modified Ad vectors carrying a stretch of lysine residues in the C-terminus of a fiber knob have been demonstrated to poorly activate innate immune responses after systemic injection, compared with conventional Ad vectors [24]. These results suggest that Ad vectors, including fiber-modified Ad vectors, would be suitable for prevention of I/R injury by delivering antioxidant genes to livers.

Among antioxidant enzymes, SOD is often used for detoxifying ROS in previous studies [8,17,25,26]. SOD catabolizes superoxide anion to H_2O_2; however, H_2O_2 is converted to hydroxyl radicals, which are extremely reactive and more toxic than other ROS. H_2O_2 should be removed to effectively reduce I/R injury. Another antioxidant enzyme, catalase, prevents the generation of hydroxyl radicals by catabolizing H_2O_2 to H_2O and O_2, suggesting that catalase is promising for prevention of I/R injury. However, there are few studies reporting therapeutic effects of catalase gene delivery on I/R injury [17,27].

In the present study, catalase-expressing Ad vectors were intravenously pre-administered to prevent I/R-induced hepatic injury. Pre-injection of catalase-expressing Ad vectors successfully prevented not only I/R-induced hepatic injury but also CCl_4-induced liver damages. Furthermore, mice receiving pre-injection of catalase-expressing Ad vectors showed improved survival rates after partial hepatectomy followed by hepatic I/R.

2. Materials and methods

2.1. Cells

A549 (a human lung adenocarcinoma epithelial cell line), HepG2 (a human hepatocellular liver carcinoma cell line), and 293 (a human embryonic kidney cell line) cells were cultured in Dulbecco's modified Eagle's medium (DMEM) supplemented with 10% fetal bovine serum under 5% CO_2 at 37 °C.

2.2. Ad vectors

Ad vectors were constructed by means of an improved *in vitro* ligation method [28–30]. Briefly, the LacZ gene, which is derived from pCMVβ (Marker Gene, Inc., Eugene, OR) and the catalase gene, which is derived from pZEOSV2-CAT (a kind gift from Dr. J. Andres Melendez, Albany Medical College, Albany, NY) [31,32] were inserted into pHMCA5, [33] creating pHMCA5-LacZ and pHMCA5-CAT, respectively. pHMCA5-LacZ and pHMCA5-CAT were then digested with I-CeuI and PI-SceI, and ligated with I-CeuI/PI-SecI-digested pAdHM4 [28], resulting in pAdHM4-LacZ and pAdHM4-CAT, respectively. To generate the viruses, PacI-digested Ad vector plasmids were transfected into 293 cells plated in a 60-mm dish with SuperFect (Qiagen, Inc., Valencia, CA) according to the manufacturer's instructions. The viruses were prepared by the standard method, then purified with $CsCl_2$ gradient centrifugation, dialyzed with a solution containing 10 mM Tris (pH7.5), 1 mM $MgCl_2$, and 10% glycerol, and stored in aliquots at −80 °C. The determinations of infectious titers and virus particle (VP) titers were accomplished using 293 cells and an Adeno-X rapid titer kit (Clontech, Mountain View, CA) and the method of Maizel et al. [34], respectively. Catalase-, or β-galactosidase-expressing fiber-modified Ad vectors carrying a stretch of lysine residues (K7 (KKKKKKK) peptide) in the C-terminus of a fiber knob, AdK7-CAT and AdK7-LacZ, respectively, were similarly prepared using pAdHM41K7 [35]. The ratios of the biological-to-particle titer were 1:20, 1:31, 1:45, and 1:39 for Ad-LacZ, AdK7-LacZ, Ad-CAT, and AdK7-CAT, respectively.

2.3. Western blot analysis for catalase expression

A549 cells were transduced with Ad vectors at 3000 VP/cell for 2 h. Forty-eight hours later, cells were harvested and lysed with lysis buffer (20 mM Tris–HCl (pH 8.0), 137 mM NaCl, 1% Triton X-100, 10% glycerol) containing protease inhibitor cocktail (Sigma Chemical., St. Louis, MO). Equal quantities of protein (5 μg), as determined by a protein assay (Bio-Rad, Hercules, CA), were subjected to sodium dodecyl sulfate/12.5% polyacrylamide gel electrophoresis (SDS-PAGE) and transferred onto a polyvinylidene fluoride membrane (Millipore, Bedford, MA). After blocking nonspecific binding, the membrane was incubated with anti-catalase antibody (diluted 1/8000; Calbiochem, San Diego, CA) at room temperature for 3 h, followed by reaction with horse radish peroxidase (HRP)-conjugated anti-rabbit IgG (diluted 1/3000; Cell Signaling Technology, Beverly, MA) at room temperature for 1 h. The band was visualized by ECL Plus Western blotting detection reagents (Amersham Bioscience, Piscataway, NJ), and the signals were read using an LAS-3000 imaging system (Fujifilm, Tokyo, Japan). For detection of the internal control, a polyclonal anti-glyceraldehyde-3-phosphate dehydrogenase antibody (diluted 1/5000; Trevigen, Gaithersburg, MD) and an HRP-conjugated anti-rabbit IgG were used.

2.4. In vitro protective effect of catalase-expressing Ad vectors on ROS-induced cell damage

HepG2 cells (5000 cells/well) were seeded onto a 96-well plate. On the following day, the cells were transduced with Ad-LacZ, AdK7-LacZ, Ad-CAT, or AdK7-CAT at 300 or 3000 VP/cell for 2 h. After a 48-h incubation, the medium was exchanged for normal medium containing 30 mM menadione (Sigma Chemical), which is a ROS inducer. On the following day, the cell viability was determined by Alamar blue staining (BioSource, San Diego, CA).

2.5. Catalase activities in the liver after intravenous administration of Ad vectors

Ad vectors (Ad-LacZ, AdK7-LacZ, Ad-CAT, and AdK7-CAT) were intravenously administered into C57BL/6 mice (7–8-week-old females; Nippon SLC, Shizuoka, Japan) at a dose of 1×10^{10} VP/mice. Forty-eight hours later, the livers were isolated and homogenized with 50 mM potassium phosphate buffer containing 1 mM EDTA. The supernatants were recovered after centrifugation of the homogenates, and catalase activity in the supernatants was measured using a CalBiochem Catalase Assay Kit (Calbiochem).

2.6. Hepatic ischemia/reperfusion experiment

Mice were intravenously administered PBS (control) or Ad vectors via the tail vein at a dose of 10^{10} VP/mice. A partial hepatic ischemia/reperfusion experiment was performed as previously described [36,37]. Briefly, 2 days post-administration of Ad vectors, mice were anesthetized with a peritoneal injection of pentobarbital sodium (50 mg/kg). An incision was made in the abdomen, and all structures in the portal triad (hepatic artery, portal vein, bile duct) were occluded with a vascular clamp for 1 h to induce hepatic ischemia. Then, blood was allowed to flow through the liver again by removal of the clamp (reperfusion). After an appropriate period of reperfusion (0, 1, 6, 24 h), blood was collected via retro-orbital bleeding, and serum was obtained by centrifugation. The aspartate aminotransferase (ALT) and alanine aminotransferase (AST) activities in serum, as indicators of liver injury during reperfusion, were assayed using a transaminase-CII test (Wako, Osaka, Japan). In separate experiments, histology in the liver sections was evaluated 24 h after reperfusion. The livers were recovered and fixed by immersion in 10% buffered formalin, embedded in paraffin and processed for histology. Tissue damage was assessed in hematoxylin and eosin-stained sections. A sham surgery was performed under anesthesia but without occluding the vessels.

2.7. CCl_4-induced liver injury experiment

Ad vectors were intravenously administered into mice as described above. Forty-eight hours after Ad vector injection, CCl_4 dissolved in olive oil was intraperitoneally administrated to the mice at a dose of 1 ml/kg body weight to induce acute liver failure. Twenty-four hours after CCl_4 administration, blood was collected via retro-orbital bleeding, and the levels of ALT and AST in the serum were determined as described above.

2.8. Partial hepatectomy

Ad vectors were intravenously administered into mice as described above. Forty-eight hours after Ad vector injection, mice were anesthetized and subjected to two-thirds hepatectomy as described previously [38,39]. Subsequently, liver I/R was conducted by occlusion of the blood vessel to block the blood flow into the remnant liver for 8 min followed by reperfusion as described above. After the surgery, the mice were maintained under conventional conditions to monitor survival rates.

2.9. Statistical analysis

Results were expressed as the means ± S.D. Statistically significant differences between groups were determined by the two-way analysis of variance, followed by Student's *t*-test. The levels of statistical significance were set at $p<0.05$ and $p<0.01$.

3. Results

3.1. Ad vector-mediated catalase expression in vitro

First, to examine *in vitro* catalase expression levels following Ad vector infection, Western blotting analysis was performed. We observed an apparent increase in the catalase expression after transduction with Ad-CAT or AdK7-CAT in A549 cells (Fig. 1). In addition, AdK7-CAT mediated higher catalase expression than Ad-CAT, probably due to the higher transduction activity of AdK7 vectors than conventional Ad vectors [35]. The control Ad vectors, Ad-LacZ and AdK7-LacZ, did not increase catalase expression, indicating that transduction with Ad vectors alone does not induce any change in the antioxidant systems.

Next, to examine whether Ad vector-mediated over-expression of catalase prevents ROS-induced cellular toxicity, the cells were incubated with 30 mM menadione following transduction with Ad vectors, and the cell viabilities were determined. It is well known that menadione produces superoxide radicals in cells, leading to oxidative stress-induced cell death [40,41]. As shown in Fig. 2, the cell viability was significantly reduced to less than 50% in the presence of 30 mM menadione. In contrast, transduction with catalase-expressing Ad vectors dramatically improved the cell viabilities. Transduction with Ad-CAT and AdK7-CAT at 300 VP/cell resulted in cell viabilities of 70.8% and 79.1% of the cell, respectively. These results indicate that Ad vector-mediated over-expression of catalase is beneficial in preventing oxidative stress-induced cell death by efficiently deleting ROS.

3.2. Catalase activity in the liver following catalase-expressing Ad vector injection

Next, to measure catalase activities in the liver following intravenous administration of Ad vectors, the livers were recovered 48 h after Ad vector injection, and catalase activities in the liver were determined. The catalase activities were 2.4-fold and 4.3-fold increased following administration of Ad-CAT and AdK7-CAT, respectively (Fig. 3). By contrast, we found no elevation in the catalase activity by LacZ-expressing Ad vectors. These results indicate that catalase activity in the liver is significantly elevated by intravenous administration of catalase-expressing Ad vectors.

3.3. Prevention of hepatic I/R injury by pre-administration of catalase-expressing Ad vectors

To evaluate the ability of catalase-expressing Ad vectors to prevent hepatic I/R injury, serum ALT and AST levels were measured after 1 h of hepatic ischemia followed by reperfusion. Both serum ALT and AST levels were highly elevated at 1 h and 6 h after the reperfusion of hepatic flows in the mice pre-injected with PBS, indicating that hepatic injury was induced by I/R (Fig. 4). At 1 h after reperfusion, the ALT and AST levels increased from 59.3 to 184.0 and from 421.2 to 1174.7 IU/L, respectively. However, pretreatment with Ad-CAT or AdK7-CAT significantly reduced the serum ALT and AST levels at 6 h after reperfusion. The ALT and AST levels in mice pre-injected with AdK7-CAT were 3.9- and 4.4-fold lower than those in mice pre-injected with PBS. Reductions in the ALT and AST levels were also observed at 1 h after reperfusion, although these changes were not statistically significant. The control Ad vectors, Ad-LacZ and AdK7-LacZ, exhibited no suppressive effects on the I/R-induced elevation of serum ALT and AST levels.

Furthermore, to histologically evaluate the preventive effects of catalase-expressing Ad vectors, liver sections were prepared 24 h after reperfusion. An extensive necrotic area was observed in the mice pretreated with PBS or AdK7-LacZ (Fig. 5B, C). In contrast, transduction with Ad-CAT or AdK7-CAT resulted in a dramatic decrease in the necrotic area induced by hepatic I/R (Fig. 5D, E). In particular,

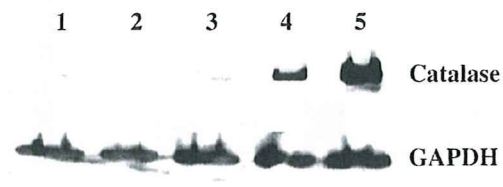

Fig. 1. Catalase expression following Ad vector transduction. A549 cells were transduced with Ad-LacZ, Ad-CAT, or AdK7-CAT at 3000 VP/cell for 2 h. Protein samples were collected after a 48-h incubation and analyzed by Western blotting. Lane 1, mock; lane 2, Ad-LacZ; lane 3, AdK7-LacZ; lane 4, Ad-CAT; lane 5, AdK7-CAT. The results are representative of two

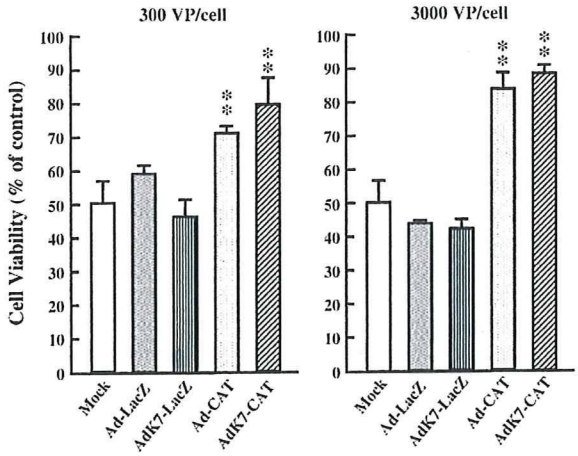

Fig. 2. Protective effects of catalase-expressing Ad vectors against menadione-induced cell death. HepG2 cells were transduced with Ad vectors at 300 or 3000 VP/cell for 2 h. After a 48-h incubation, menadione was added to the medium at a final concentration of 30 mM, and the cells were cultured for an additional 24 h. The cellular viabilities were then determined by Alamar blue staining. The cellular viabilities were normalized to the viability of Ad vector-infected HepG2 cells in the absence of menadione. The data are expressed as the means ± S.D. ($n = 4$). **Significantly different from the mock-infected group at $p < 0.01$.

pre-injection of AdK7-CAT almost completely prevented necrosis in the liver, although there were several small necrotic areas in the liver pretreated with Ad-CAT, probably due to the higher transduction efficiency and less liver toxicity profile of AdK7 vectors in the liver compared with conventional Ad vectors [24]. A TUNEL assay indicated that Ad-CAT and AdK7-CAT prevented the DNA fragmentation caused by hepatic I/R in hepatocytes (data not shown). These results indicate that the I/R-induced histological damages were also significantly attenuated by pretreatment with catalase-expressing Ad vectors.

3.4. Preventive effect of catalase-expressing Ad vectors on CCl_4-induced liver injury

To explore whether Ad vector-mediated catalase expression prevents other types of oxidative stress-induced liver injury, CCl_4 was intraperitoneally injected into mice pretreated with catalase-expressing Ad vectors. CCl_4 is well known to produce CCl_3 radical, leading to acute liver injury. Serum ALT and AST levels were highly elevated following CCl_4 treatment in mice pretreated with PBS or LacZ-expressing Ad vectors (Fig. 6). However, serum ALT and AST levels were markedly reduced by pretreatment with Ad-CAT and AdK7-CAT. AdK7-CAT mediated a 4.9-fold and 3.9-fold reduction in serum ALT and AST levels, respectively, compared with PBS. Ad-CAT and AdK7-CAT also mediated a dramatic improvement of CCl_4-induced gross abnormality in the liver (data not shown). These results indicate that catalase-expressing Ad vectors possess preventive effects on oxidative stress-induced injury that are distinct from their effects on I/R injury.

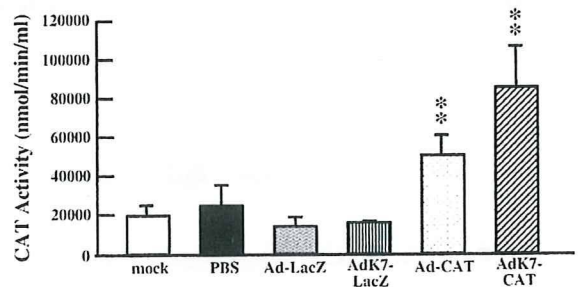

Fig. 3. Catalase activity in the liver following intravenous administration of catalase-expressing Ad vectors. Ad vectors were administered to mice at the dose of 1×10^{10} VP/mouse. The livers were recovered 48 h after injection, and catalase activities in mouse liver homogenates were determined. The data are expressed as the means ± S.D. ($n = 5$). **Significantly different from the mock-infected group at $p < 0.01$.

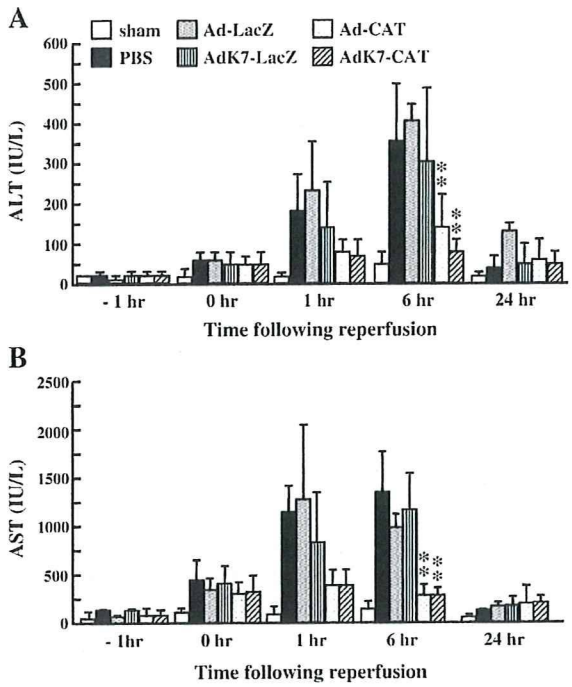

Fig. 4. Effects of pre-administration of catalase-expressing Ad vectors on serum ALT (A) and AST (B) levels in mice following hepatic ischemia/reperfusion injury. Ad vectors were intravenously administered to mice at a dose of 1×10^{10} VP/mice. Forty-eight hours after Ad vector injection, mice were subjected to a 1 h period of ischemia followed by hepatic reperfusion. Serum samples were taken at 1 h before ischemia, and 0, 1, 6, and 24 h after reperfusion. The data are expressed as the mean ± S.E. ($n = 3$–8). **Significantly different from the PBS-injected group at $p < 0.01$.

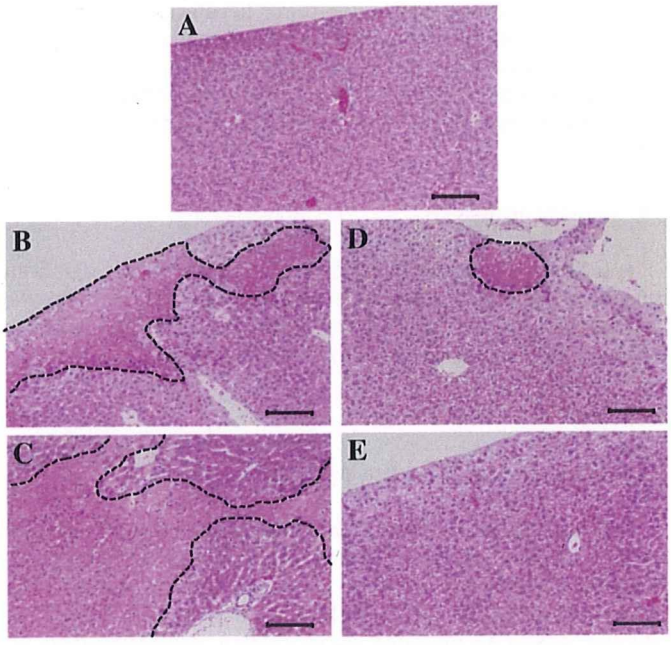

Fig. 5. Representative images of liver sections of mice 24 h following hepatic ischemia/reperfusion. A) Sham, B) PBS, C) AdK7-LacZ, D) Ad-CAT, and E) AdK7-CAT. Mice were subjected to hepatic I/R 48 h after Ad vector injection, as described in Fig. 4. Livers were recovered 24 h after I/R treatment, and liver sections stained with hematoxylin and eosin were observed under a microscope. A dashed line indicates the necrotic area. The scale bar represents 100 μm.